Perinatal changes in cardiac geometry and function in growth restricted fetuses at term

Olga Patey*†‡, Julene S Carvalho*†‡§ and Basky Thilaganathan*†§

Molecular & Clinical Sciences Research Institute, St George's University of London*;

Fetal Medicine Unit, St. George's University Hospitals NHS Foundation Trust, London†;

Brompton Centre for Fetal Cardiology, Royal Brompton Hospital, London‡;

Joint last authors§

Author for correspondence: Dr Olga Patey

Address: Fetal Medicine Unit

4th Floor, Lanesborough Wing

St. George's University Hospitals NHS Foundation Trust

London SW17 0QT

Email: pateyolga@gmail.com

Short version of title: Perinatal heart in FGR

Keywords: fetal echocardiography; fetal heart; fetal growth restriction; fetal hypoxemia; speckle tracking; tissue Doppler imaging; left ventricular torsion.

ABSTRACT

Objective To evaluate the effect of fetal growth restriction (FGR) at term on fetal and neonatal cardiac geometry and function.

Methods Prospective study of 87 pregnant women delivering, comprising of 54 normally grown and 33 FGR pregnancies at term. Fetal and neonatal conventional, spectral tissue Doppler, and 2D speckle tracking imaging echoes were performed few days before and within hours of birth.

Results Compared to normal pregnancy, FGR fetuses exhibited more globular ventricular geometry, poorer myocardial deformation and cardiac function (LV sphericity index [SI]: 0.49 vs 0.54, RV SI: 0.54 vs 0.60, LV torsion 3.0deg/cm vs 1.6deg/cm, LV isovolumetric contraction time normalised by cardiac cycle length: 104ms vs 121ms, intra-ventricular septum E'/A': 0.71 vs 0.60, $p<0.001$ for all). The poorest adverse perinatal outcomes occurred in FGR fetuses with most impaired cardiac functional indices. When compared to normal newborns, FGR neonates revealed persistent alteration in cardiac parameters (LV SI: 0.50 vs 0.53, RV SI: 0.44 vs 0.54, LV torsion 1.4deg/cm vs 1.1deg/cm, LV myocardial performance index [MPI'] 0.42 vs 0.52, $p<0.001$ for all). Paired comparison of fetal and neonatal cardiac indices in FGR demonstrated that birth resulted in significant improvement in some, but not all cardiac indices (RV SI: 0.60 vs 0.54, RV MPI': 0.49 vs 0.39, $p<0.001$ for all).

Conclusions Compared to normal pregnancy, FGR fetuses and neonates at term exhibit altered cardiac indices indicative of myocardial impairment that reflect adaptation to placental hypoxemia and alterations in hemodynamic load around the time of birth. Elucidating potential mechanisms that contribute to the alterations in perinatal cardiac adaptation in FGR could improve the management and evolve better therapeutic strategies to reduce the risk of adverse pregnancy outcome.

INTRODUCTION

Fetal growth restriction (FGR) and hypoxemia of placental insufficiency affect 5% to 10% of pregnancies (1). Previous animal (2, 3) and human studies (4, 5) have shown that FGR is associated with adverse impact on fetal and long-term cardiovascular function, but the direct effects of fetal hypoxemia on acute changes in perinatal cardiac transition remain largely unexplored. Subclinical myocardial changes in FGR term fetuses and neonates might still have a detrimental impact on the burden of disease and increase the risk of cardiovascular morbidity and mortality in later life (5, 6). Only two small cross-sectional retrospective studies have demonstrated persistence of cardiac dysfunction from fetal life into childhood (5, 6). There are no prospective data exploring fetal perinatal cardiac adaptation in FGR. Furthermore, modern cardiac imaging modalities, such as tissue Doppler and speckle tracking have fundamentally changed characterization of myocardial function and have been shown to demonstrate a higher sensitivity for detecting even mild myocardial damage and established a stronger predictive value for subsequent cardiovascular complications compared to conventional echo indices (7, 8). However, there is a paucity of data using these novel methods in the assessment of perinatal heart function in FGR. The aim of this study was to examine the effect of FGR at term on fetal and neonatal cardiac geometry, myocardial deformation and LV torsion.

SUBJECTS AND METHODS

Study population

This was a prospective longitudinal study of 87 pregnant women delivering at term that included 54 pregnancies with a normal outcome and 33 pregnancies affected by FGR. Pregnant women attending for routine antenatal care in the Fetal Medicine Unit at St. George's University Hospitals NHS Foundation Trust between February 2014 and June 2016 were recruited if the fetuses had normal cardiac anatomy and there was no maternal or pregnancy-related co-morbidity. FGR was defined as estimated fetal weight below 10th centile with Doppler evidence of placental dysfunction (9). Exclusion criteria were a fetal structural and chromosomal abnormality, adverse pregnancy outcome (other than related to FGR) and pregnant women in labour. All participants gave written informed consents for fetal and neonatal cardiac assessment. The Ethics Committee of NRES Committee London-Surrey Borders approved the study protocol (Reference -12/LO/0945).

Echocardiography

Fetal B-mode, M-mode, spectral pulsed-wave (PW) Doppler, spectral tissue Doppler imaging (PW-TDI) and speckle tracking imaging (STI) echocardiograms were performed few days before birth. The neonatal cardiac assessment was conducted within hours after birth. One investigator (OP) performed all fetal and neonatal ultrasound examinations using a Vivid E9 ultrasound system (General Electric, Norway). Fetal M-mode, B-mode, and PW Doppler measurements were made with the convex array obstetric transducer 4C, while the paediatric /neonatal cardiac sector probe 12S was used for neonatal heart examination. PW-TDI curves and 2D images for STI analysis were obtained and recorded in the same manner and with the same ultrasound transducer (adult linear transducer M5S) in both fetal and neonatal groups.

M-mode ultrasound was used for assessment of cardiac geometry and function and ventricular longitudinal axis annular motion. *B-mode imaging* was performed for obtaining measurements of ventricular chambers, valve dimensions, and both LV and RV sphericity indices calculated by dividing ventricular end-diastolic dimension (EDD) by end-diastolic length (EDL) for each ventricle (10). *PW Doppler technique* was used to obtain Doppler signals from the inflow and outflow tracts for evaluation of diastolic and systolic function respectively and calculation of LV and RV stroke volume (SV) and cardiac output (CO). *PW-TDI technique* was applied to derive cardiac indices of myocardial motion in systole and diastole and was also used for estimation of LV and RV MPI'. *Speckle tracking imaging (STI*) was used to derive myocardial deformation indices (longitudinal, circumferential, radial and rotational) with frame rate *greater than 100 frames per second (fps)*. All echocardiographic measurements were performed in a single beat according to the standardised protocol of the study and with regards to previously described fetal echo techniques (11). Several digital clips were obtained, serially numbered and *anonymised* patient data was then transferred to the dedicated software EchoPAC (version 112, GE Medical System) for further analysis. LV net twist was calculated by subtracting the peak basal rotation from the peak apical rotation. LV torsion was considered as a result of net twist divided by the LV end-diastolic length. Considering variations of fetal position, it is crucial to correctly identify the direction of the fetal LV rotation at LV short axis basal and apical levels. Speckle tracking analysis of rotational direction was adjusted with respect to the fetal orientation on the ultrasound screen. The time-interval values were adjusted by cardiac cycle length normalising for the difference in heart rate. Other fetal and neonatal indices were normalised by dividing corresponding measurements by the ventricular length or end-diastolic dimension according to study methodology (Supplementary materials) with regards to previous recommendations (12-14).

Intra- and inter-observer reproducibility

The same observer (OP) repeated TDI and STI measurements of 25 fetal and 25 neonatal echoes in a different cardiac cycle of GE Vivid E9 ultrasound system (for TDI indices) and vendor-specific EchoPAC software (for STI indices). In randomly chosen ten fetal and ten neonatal echocardiograms, two different observers (MB and VDZ) repeated TDI and STI measurements in a different cardiac cycle (blinded to each other's measurements). Both, limits of agreement (LoA) with Bland-Altman graphs/Pitman's test of difference in variance, and intra-class correlation coefficient (ICC) were calculated.

Statistical analysis

Sample size and power calculations were performed based on our pilot data (11). For strain rate as a primary outcome, a sample of 66 pregnancies (33 normal and 33 FGR) would detect a rate of change (length/s) difference of 0.21 (equivalent to 10% of the mean, 2.05), with power of 85%, significance level of 5%, and assuming a standard deviation of 0.28. To allow for possible confounding factors including dropouts, this number was increased to 87 pregnancies. Statistical analysis was performed using SPSS version 22.0 (SPSS Inc., Chicago, IL, USA). Both Shapiro-Wilk test and Kolmogorov-Smirnov test were performed to assess the data for normality. For normally distributed data, paired T-test and independent sample T-tests to compare fetal and neonatal cardiac variables were performed. For skewed data, Wilcoxon sign rank and Mann-Whitney tests were used as appropriate. The differences between groups were deemed as significant only if the 2-tailed p-values were less than 0.01 (Bonferroni correction for type 1 error or false positive results of multiple measurements). Additionally, a linear regression analysis was used to examine the relationship between LV rotational parameters and fetal/neonatal selected cardiac indices.

RESULTS

A total of 87 women consented to the study (54 normal and 33 FGR pregnancies). Of those, deformational data in basal/apical four-chamber views were obtained in 86 fetuses and 80 neonates, and short axis view data were available in 80 fetuses and 80 neonates. Maternal demographic characteristics and scan details of the pregnancies enrolled in the study are summarised in Table 1.

Cardiac geometry

FGR fetuses demonstrated significantly decreased RV/LV end-diastolic dimension (EDD) ratios, RAVV/LAVV diameter ratios, LV and IVS wall thickness and a significant increase in RV wall thickness and LV and RV sphericity indices when compared to normal pregnancy. Postnatally, FGR neonates exhibited persistence of significantly increased LV and RV sphericity indices, RV/LV EDD and RAVV/LAVV ratios, and thickening of the interventricular septum (Figure 1, Table 2 and Table S1). Perinatal changes in the FGR group showed a significant improvement in some parameters, with an increase in RV end-diastolic length (EDL) resulting in decreased RV sphericity index.

Global myocardial deformation and performance

FGR fetuses had significantly higher LV and RV longitudinal strain/strain rate and significantly lower LV torsion values compared to normal fetuses. After birth, there was persistence of significantly increased LV and RV longitudinal strain, LV strain rate, LV and RV MPI', and significantly reduced LV torsion in the FGR neonates (Figure 2, Table 2 and Table S1). Perinatal changes in FGR neonates showed significant improvement in all indices of myocardial deformation as well as LV and RV MPI'.

Systolic function

PW-TDI results demonstrated a significant increase in LV, RV, and IVS myocardial annular systolic velocities S' consistent with speckle tracking findings of increased longitudinal contractility in FGR fetuses (Table 2 and Table S1). There was also a significant increase in LV isovolumetric contraction time' (IVCT') period in FGR fetuses. Postnatally, there were significantly increased LV CO, IVS S', and both LV and RV IVCT', while RV ejection time' was reduced in FGR neonates. Perinatal changes in FGR neonates showed significant improvement with increased LV CO and reduced LV and RV IVCT' (Table 2 and Table S1).

Diastolic function

Compared to the normal group, FGR fetuses had a significant decrease in IVS E'/A' ratio and prolonged LV and RV isovolumetric relaxation time' (IVRT'). In the FGR neonates, there was persistence of decreases in LV and RV diastolic inflow velocity ratio (E/A <1), E'/A' ratios (E'/A'<1), RV and LV relaxation time, whereas LV and RV IVRT' were prolonged (Table 2 and Table S1). LV torsion values were significantly lower in FGR fetal and neonatal groups compared to normal pregnancy (Table S1). Importantly, four FGR fetuses with the lowest values of LV torsion also had altered geometrical indices (more globular heart) and impaired systolic and diastolic indices (Figure 3) and required admission to the neonatal intensive care unit immediately after birth, with one resulting in perinatal death. Summary of alterations in cardiac parameters in FGR term fetus and neonates compared to normal groups is presented in Table 3 and Figure 4.

Reproducibility

The limits of agreement (LoA) and intra-class correlation coefficient (ICC) showed excellent intra- and inter-observer agreement of all fetal and neonatal TDI and STI indices (ICC=0.8-0.9). Radial deformation showed moderate correlation and excellent agreement (Table S2).

DISCUSSION

This study presents a comprehensive paired analysis of cardiac geometric and functional parameters in FGR fetuses and neonates. The findings show that FGR fetuses exhibit more globular hearts, thinner LV wall chambers, hypertrophied RV, increased longitudinal myocardial contractility, reduced LV torsion and diastolic dysfunction with evidence of persistence of some of these alterations after birth. The antenatal cardiac observations were related to adverse perinatal outcome and likely to reflect the deleterious effect of placental hypoxemia on the fetal myocardium and partial recovery with changes in volume and resistance loading conditions at birth.

Fetal cardiac geometry and function

LV and RV sphericity indices demonstrated that FGR fetuses at term exhibit a more 'globular heart' with shorter ventricles compared to normal fetuses. The left ventricle also had thinner LV walls while the right ventricle was more hypertrophied with less pronounced RV dominance. These findings could be attributed to the effect of fetal hypoxemia, which is characterized by a preferential redistribution of the blood flow towards the left ventricle to favour perfusion of the fetal heart, adrenal glands, and brain – so-called "brain sparing" effect (15). Cerebral vasodilatation leads to a decrease in LV afterload while increased placental vascular resistance increases RV afterload (16). Considerable animal data provide supportive evidence that prenatal exposure to hypoxia can lead to cardiomyocyte hypertrophy, myocardial hypoplasia, reduced cell number due to increased cell death (apoptosis), decreased myocyte proliferation and increased the collagen deposition and fibrosis (2, 3, 17-19). A natural consequence of a chronic pressure overload is ventricular hypertrophy, while

volume overload leads to ventricular cavity dilatation and wall thinning (20). In agreement with our findings, others have also reported a more globular remodelled heart in preterm FGR fetuses (21, 22). There was a significant increase in LV and RV longitudinal strain and strain rate as well as myocardial systolic velocities in the FGR group that are likely to reflect the impact of loading conditions on myocardial contractility (23). It would suggest that increased longitudinal myocardial deformation is required under hypoxemic conditions to maintain the same cardiac output as normal term fetuses (24). Our findings of enhanced cardiac performance and unchanged cardiac output are in concordance with experimental fetal sheep and human data during progressively worsening hypoxemia (25), predisposing to myocardial cell damage, local fibrosis and myocyte death (26). Torsion facilitates uniform distribution of LV stress and fibre shortening across the wall (27). The observed decrease in torsion would increase endocardial stress and strain and, as a consequence, increase oxygen demand and reduce the efficiency of LV diastolic function (27). The strong association between increased LV sphericity, reduced LV torsion and diminished apical systolic rotation has also previously been demonstrated in adult populations (28). Lower LV torsional deformation values in FGR fetuses, predispose to reduced LV diastolic function (27) with a subsequent increase in endocardial stress and oxygen demand. In keeping with this, FGR fetuses had increased LV and RV isovolumetric relaxation time intervals and decreased IVS E'/A' ratio, reflecting impaired diastolic function (21).

Neonatal cardiac geometry and function

FGR neonates demonstrated the increased LV and RV sphericity index and RV/LV end-diastolic ratio indicating persistence of 'a globular heart' compared to normal neonates. FGR newborns revealed an increased LV cardiac output, IVS longitudinal contractility, and LV and RV longitudinal myocardial deformation. However, both LV and RV MPI' were increased as

a result of prolonged LV and RV IVCT' and IVRT' intervals and reduced RV ejection time'. The geometrical and functional differences with tricuspid regurgitation in the majority of observed FGR neonates are most likely the result of persistence of prenatal alterations of cardiac geometry due to the intrauterine state of chronic hypoxia and altered haemodynamic load at birth (4). Elevated biventricular longitudinal contractility observed in our study can be attributed to a compensatory cardiac adaptation to generate a sufficient cardiac output in presence of chamber dilatation and altered myocardial architecture. The observation of diastolic dysfunction is consistent with previous studies reporting geometrical alterations and cardiac dysfunction in FGR newborns (4, 29, 30). Reduced LV torsion in FGR neonates is likely to be a consequence of residual fetal LV chamber dilatation and increased LV longitudinal myocardial deformation and would contribute to diastolic dysfunction observed in the first hours after birth.

Perinatal changes in LV/RV sphericity and LV/RV IVCT' intervals in FGR have similar trends as previously reported in normal fetuses and neonates (11). Additionally, our perinatal results revealed the presence of LV impaired relaxation (E/A and E'/A' ratios <1) in FGR neonates with a significant increase in LV E/E' ratio that is indicative of persistence of LV diastolic dysfunction in the first hours after birth.

Strength and limitations

The main strength of the present study was its prospective follow-up design and the inclusion of a healthy and pathological (FGR) study population where the impact of birth - a natural intervention - was studied longitudinally. Strict methodology and the same manner of fetal and neonatal cardiac assessment confirmed by good intra- and inter-observer repeatability insured the plausibility of our findings. Although, the intra- and inter-observer agreement in this study was high, time and training are essential to acquire high quality images necessary

for fetal TDI and STI measurements, performing analysis and interpretation before implementation of these technique into clinical routine. The limitation of our study was a proportionately small number of FGR pregnancies (n=33) included; however, the study power was sufficient to demonstrate significant alterations in cardiac parameters in this study group.

Conclusion

In summary, growth-restricted fetuses exhibit altered cardiac indices indicative of myocardial impairment and ventricular dysfunction that are likely to reflect the effect of hypoxemia from uteroplacental insufficiency. Improvement in the some of these cardiac indices in FGR neonates occurred at birth reflective of changes in haemodynamic load. Understanding the potential mechanisms of cardiac findings in FGR fetuses may provide insights on perinatal adaptation and failure of these adaptive responses in pathological pregnancies.

Clinical perspectives

Evidence of persistent changes in ventricular geometry and function in the first days after birth may signal a predisposition to longer-term cardiovascular morbidity in FGR offspring. It would be of great interest to assess whether these geometrical and functional alterations persist through infancy and the long-term outcome of our study neonates in later childhood. Our results may also be of relevance in optimizing the perinatal outcomes of FGR pregnancy using the fetal period as a potential window for future intervention.

ACKNOWLEGEMENTS

We thank the General Electric Ultrasound Company for providing the ultrasound platform and EchoPAC software for this research, all patients that have taken part in this study, Dr Margarita Bartsota and Miss Vahideh Davatgar Zahiri for helping with reproducibility study measurements, and medical staff of the Fetal Medicine Unit, St. George's University Hospital for their contribution to patient's recruitment.

CONFLICT OF INTERESTS

The authors report no conflict of interest.

FUNDING SOURCES

OP was partly supported by Children's Heart Unit Fund (CHUF), Royal Brompton and Harefield Hospital Charity [registration number 1053584] and SPARKS charity (registered no.1003825, grant ref. no.14EDI01).

REFERENCES

1. Figueras F, Gratacos E. Stage-based approach to the management of fetal growth restriction. *Prenat Diagn*. 2014; **34**: 655-659.

2. Tintu A, Rouwet E, Verlohren S, Brinkmann J, Ahmad S, Crispi F, van Bilsen M, Carmeliet P, Staff AC, Tjwa M, Cetin I, Gratacos E, Hernandez-Andrade E, Hofstra L, Jacobs M, Lamers WH, Morano I, Safak E, Ahmed A, le Noble F. Hypoxia induces dilated cardiomyopathy in the chick embryo: mechanism, intervention, and long-term consequences. *PLoS One*. 2009; **4**: e5155.

3. Tong W, Xue Q, Li Y, Zhang L. Maternal hypoxia alters matrix metalloproteinase expression patterns and causes cardiac remodeling in fetal and neonatal rats. *Am J Physiol Heart Circ Physiol*. 2011; **301**: H2113-2121.

4. Crispi F, Bijnens B, Figueras F, Bartrons J, Eixarch E, Le Noble F, Ahmed A, Gratacos E. Fetal growth restriction results in remodeled and less efficient hearts in children. *Circulation*. 2010; **121**: 2427-2436.

5. Cruz-Lemini M, Crispi F, Valenzuela-Alcaraz B, Figueras F, Sitges M, Bijnens B, Gratacos E. Fetal cardiovascular remodeling persists at 6 months in infants with intrauterine growth restriction. *Ultrasound Obstet Gynecol*. 2016; **48**: 349-356.

6. Cruz-Lemini M, Crispi F, Valenzuela-Alcaraz B, Figueras F, Gomez O, Sitges M, Bijnens B, Gratacos E. A fetal cardiovascular score to predict infant hypertension and arterial remodeling in intrauterine growth restriction. *Am J Obstet Gynecol*. 2014; **210**: 552 e551-552 e522.

7. Comas M, Crispi F, Cruz-Martinez R, Martinez JM, Figueras F, Gratacos E. Usefulness of myocardial tissue Doppler vs conventional echocardiography in the evaluation of cardiac dysfunction in early-onset intrauterine growth restriction. *Am J Obstet Gynecol*. 2010; **203**: 45 e41-47.

8. Crispi F, Bijnens B, Sepulveda-Swatson E, Cruz-Lemini M, Rojas-Benavente J, Gonzalez-Tendero A, Garcia-Posada R, Rodriguez-Lopez M, Demicheva E, Sitges M, Gratacos E. Postsystolic shortening by myocardial deformation imaging as a sign of cardiac adaptation to pressure overload in fetal growth restriction. *Circ Cardiovasc Imaging*. 2014; **7**: 781-787.

9. Gordijn SJ, Beune IM, Thilaganathan B, Papageorghiou A, Baschat AA, Baker PN, Silver RM, Wynia K, Ganzevoort W. Consensus definition for placental fetal growth restriction: a Delphi procedure. *Ultrasound Obstet Gynecol*. 2016; **48**: 333-339.

10. Brooks PA, Khoo NS, Hornberger LK. Systolic and diastolic function of the fetal single left ventricle. *J Am Soc Echocardiogr*. 2014; **27**: 972-977.

11. Patey O, Gatzoulis MA, Thilaganathan B, Carvalho JS. Perinatal Changes in Fetal Ventricular Geometry, Myocardial Performance, and Cardiac Function in Normal Term Pregnancies. *J Am Soc Echocardiogr*. 2017; **30**: 485-492.e485.

12. Lorch SM, Ludomirsky A, Singh GK. Maturational and growth-related changes in left ventricular longitudinal strain and strain rate measured by two-dimensional speckle tracking echocardiography in healthy pediatric population. *J Am Soc Echocardiogr*. 2008; **21**: 1207-1215.

13. Cruz-Lemini M, Crispi F, Valenzuela-Alcaraz B, Figueras F, Sitges M, Gomez O, Bijnens B, Gratacos E. Value of annular M-mode displacement vs tissue Doppler velocities to assess cardiac function in intrauterine growth restriction. *Ultrasound Obstet Gynecol*. 2013; **42**: 175-181.

14. Patey O. Re: Differential effect of assisted reproductive technology and small-for-gestational age on fetal cardiac remodeling. B. Valenzuela-Alcaraz, F. Crispi, M. Cruz-Lemini, B. Bijnens, L. Garcia-Otero, M. Sitges, J. Balasch and E. Gratacos. Ultrasound Obstet Gynecol 2017; 50: 63-70. *Ultrasound Obstet Gynecol*. 2017; **50**: 17-18.

15. Garcia-Canadilla P, Rudenick PA, Crispi F, Cruz-Lemini M, Palau G, Camara O, Gratacos E, Bijnens BH. A computational model of the fetal circulation to quantify blood redistribution in intrauterine growth restriction. *PLoS Comput Biol*. 2014; **10**: e1003667.

16. Makikallio K, Vuolteenaho O, Jouppila P, Rasanen J. Ultrasonographic and biochemical markers of human fetal cardiac dysfunction in placental insufficiency. *Circulation*. 2002; **105**: 2058-2063.

17. Ream M, Ray AM, Chandra R, Chikaraishi DM. Early fetal hypoxia leads to growth restriction and myocardial thinning. *Am J Physiol Regul Integr Comp Physiol*. 2008; **295**: R583-595.

18. Thompson JA, Piorkowska K, Gagnon R, Richardson BS, Regnault TR. Increased collagen deposition in the heart of chronically hypoxic ovine fetuses. *J Dev Orig Health Dis*. 2013; **4**: 470-478.

19. Evans LC, Liu H, Pinkas GA, Thompson LP. Chronic hypoxia increases peroxynitrite, MMP9 expression, and collagen accumulation in fetal guinea pig hearts. *Pediatr Res*. 2012; **71**: 25-31.

20. Toischer K, Rokita AG, Unsold B, Zhu W, Kararigas G, Sossalla S, Reuter SP, Becker A, Teucher N, Seidler T, Grebe C, Preuss L, Gupta SN, Schmidt K, Lehnart SE, Kruger M, Linke WA, Backs J, Regitz-Zagrosek V, Schafer K, Field LJ, Maier LS, Hasenfuss G. Differential cardiac remodeling in preload versus afterload. *Circulation*. 2010; **122**: 993-1003.

21. Perez-Cruz M, Cruz-Lemini M, Fernandez MT, Parra JA, Bartrons J, Gomez-Roig MD, Crispi F, Gratacos E. Fetal cardiac function in late-onset intrauterine growth restriction vs small-for-gestational age, as defined by estimated fetal weight, cerebroplacental ratio and uterine artery Doppler. *Ultrasound Obstet Gynecol*. 2015; **46**: 465-471.

22. Rodriguez-Lopez M, Cruz-Lemini M, Valenzuela-Alcaraz B, Garcia-Otero L, Sitges M, Bijnens B, Gratacos E, Crispi F. Descriptive analysis of the different phenotypes of cardiac remodeling in fetal growth restriction. *Ultrasound Obstet Gynecol*. 2016.

23. Bauer F, Jamal F, Douillet R, Le Roi F, Bouchoule I, Bizet-Nafeh C, Godin M, Cribier A, Derumeaux G. [Acute changes in load: effects of myocardial velocities measured by doppler tissue imaging]. *Arch Mal Coeur Vaiss*. 2001; **94**: 1155-1160.

24. Giussani DA. The fetal brain sparing response to hypoxia: physiological mechanisms. *J Physiol*. 2016; **594**: 1215-1230.

25. Junno J, Bruun E, Gutierrez JH, Erkinaro T, Haapsamo M, Acharya G, Rasanen J. Fetal sheep left ventricle is more sensitive than right ventricle to progressively worsening hypoxemia and acidemia. *Eur J Obstet Gynecol Reprod Biol*. 2013; **167**: 137-141.

26. Iruretagoyena JI, Gonzalez-Tendero A, Garcia-Canadilla P, Amat-Roldan I, Torre I, Nadal A, Crispi F, Gratacos E. Cardiac dysfunction is associated with altered sarcomere ultrastructure in intrauterine growth restriction. *Am J Obstet Gynecol*. 2014; **210**: 550.e551-557.

27. Sengupta PP, Tajik AJ, Chandrasekaran K, Khandheria BK. Twist mechanics of the left ventricle: principles and application. *JACC Cardiovasc Imaging*. 2008; **1**: 366-376.

28. van Dalen BM, Kauer F, Vletter WB, Soliman OI, van der Zwaan HB, Ten Cate FJ, Geleijnse ML. Influence of cardiac shape on left ventricular twist. *J Appl Physiol (1985)*. 2010; **108**: 146-151.

29. Altin H, Karaarslan S, Karatas Z, Alp H, Sap F, Baysal T. Evaluation of cardiac functions in term small for gestational age newborns with mild growth retardation: a serial conventional and tissue Doppler imaging echocardiographic study. *Early Hum Dev*. 2012; **88**: 757-764.

30. Fouzas S, Karatza AA, Davlouros PA, Chrysis D, Alexopoulos D, Mantagos S, Dimitriou G. Neonatal cardiac dysfunction in intrauterine growth restriction. *Pediatr Res*. 2014; **75**: 651-657.

Table 1 Demographic characteristic of the study population

Parameter	Normal (n=54)	FGR (n=33)	P value
Maternal characteristics			
Maternal age (years)	33 (5)	32 (5)	0.221
Ethnicity: Caucasian	35 (65%)	16 (41%)	0.319
Asian	15 (28%)	13 (39%)	
Afro-Caribbean	4 (7%)	4 (12%)	
Delivery mode (Caesarean section)	14 (26%)	9 (27%)	0.424
Fetal cardiac assessment			
Gestational age (weeks)	39 (1)	38 (1)	0.665
Time gap between the fetal scan and birth (days)	10 (7)	9 (10)	0.223
Neonatal cardiac assessment			
Baby's age at the time of scan (days)	0.5 ± 0.8	0.4 ± 1.2	0.216
Baby's sex (male)	28 (52%)	15 (46%)	0.133
Baby's weight (kg)	3.516 (0.605)	2.750 (0.600)	<0.0001
Patent foramen ovale presence	54 (100%)	33 (100%)	0.376
Patent ductus arteriosus presence	43 (79%)	28 (85%)	0.564
Mild tricuspid regurgitation	3 (6%)	17 (52%)	<0.0001
Pregnancy outcome			
Admission to neonatal NICU	0 (0%)	4 (12%)	0.085
Perinatal death	0 (0%)	1 (3%)	0.276

Values are mean ± SD, median (interquartile range), or n (%); NICU, neonatal intensive care unit.

Table 2 Perinatal changes in cardiac geometry and function in FGR term fetuses and neonates compared to normal groups

Parameters	Fetus at term		Neonate	
	Normal	FGR	Normal	FGR
Cardiac geometry				
RAVV/LAVV ratio	1.18 (0.21)	1.07 (0.17)*	0.97 (0.08)	1.09 (0.19)*
LV EDL, mm	29.25 ± 4.99	25.30 ± 4.95*	33.65 ± 3.26	27.56 ± 4.13*
RV EDL, mm	30.30 (6.80)	24.90 (6.90)*	32.20 ± 3.28	26.47 ± 3.64*§
LV EDD, mm	14.08 ± 2.14	13.78 ± 2.21	16.83 ± 1.65	14.46 ± 1.94*
RV EDD, mm	16.78 ± 1.77	14.72 ± 2.44*	13.89 ± 1.54	14.19 ± 1.93‡
RV/LV EDD ratio	1.20 (0.21)	1.08 (0.20)*	0.86 (0.12)	1.00 (0.07)*
IVS thickness, mm	0.23 (0.05)	0.18 (0.06)*****	0.17 (0.04)	0.19 (0.04)*****
Global myocardial performance				
LV MPI'	0.54 (0.14)	0.55 (0.10)	0.42 (0.11)	0.52 (0.09)*‡
RV MPI	0.52 (0.13)	0.49 (0.09)	0.34 (0.06)	0.39 (0.80)*‡
Systolic function				
Heart rate	137 ± 10	140 ± 8	115 (18)	119 (22)‡
LV CO, ml/min/kg	197 (75)	195 (106)	270 ± 59	312 ± 102†‡
RV CO, ml/min/kg	213 (73)	202 (120)	208 (68)	224 (50)§
IVS S', cm/s	0.14 (0.18)	0.16 (0.07)†	0.14 (0.05)	0.16 (0.05)†
RV S', cm/s	0.18 (0.10)	0.24 (0.09)*	0.20 (0.08)	0.22 (0.08)
LV IVCT', ms	104 (26)	121 (21)*	78 ± 17	93 ± 21*‡
RV IVCT', ms	104 ± 31	105 ± 17	70 (19)	81 (27)*‡

Diastolic function

LV E/A (PW Doppler)	0.78 ± 0.11	0.79 ± 0.10	1.24 (0.20)	0.87 (0.14)*
RV E/A (PW Doppler)	0.78 (0.19)	0.79 (0.20)	1.00 (0.25)	0.85 (0.23)*
LV E'/A'	0.77 (0.24)	0.75 (0.22)	1.23 (0.27)	0.84 (0.24)*
LV E/E'	7.07 (2.14)	7.3 (2.72)	8.79 (3.36)	9.10 (3.20)‡
IVS E'/A'	0.71 (0.14)	0.60 (0.24)†	1.00 (0.4)	0.75 (0.26)*
LV IVRT', ms	101 (0.25)	118 (35)†	76 (22)	88 (29)†‡
RV IVRT', ms	106 (16)	119 (18)†	71 (18)	87 (33)*§

Values are mean ± SD and median (interquartile range). Values are normalised by ventricular length or cardiac cycle length as where appropriate. The wall thickness values are normalised by end-diastolic ventricular dimensions; FGR, fetal growth restriction; RAVV, right atrioventricular valve; LAVV, left atrioventricular valve; EDD, end-diastolic dimension; EDL, end-diastolic length; MPI', myocardial performance index; CO, cardiac output; E, early diastolic peak velocity derived by PW Doppler; A, atrial contraction diastolic peak velocity derived by PW Doppler; E', early diastolic myocardial peak velocity derived by PW-TDI; A', atrial contraction myocardial diastolic peak velocity, derived by PW TDI; IVCT', isovolumetric contraction time obtained by PW-TDI; IVRT', isovolumetric relaxation time obtained by PW-TDI; *, p-value < 0.001 and †, p-value <0.01 compared FGR fetuses and neonates with normal groups; ‡, p-values < 0.001 and §, p-value <0.01 compared FGR fetus with FGR neonate.

Table 3 Summary of alterations in cardiac parameters in FGR term fetus and neonates compared to normal groups

Cardiac geometry	Myocardial deformation	Systolic function	Diastolic function
FGR term fetuses compared to Normal fetuses			
More globular LV and RV Wider LV ↓Thickness of LV and IVS ↑Thickness of RV wall	↑LV and RV L-S ↑LV and RV L-SR ↓LV torsion	↑LV and RV S' ↑IVS S' ↑LV IVCT'	↑LV and RV IVRT' ↓IVS E'/A' (<1)
FGR neonates compared to Normal neonates			
More globular LV and RV Wider RV ↑Thickness of IVS	↑LV and RV L-S ↑LV L-SR ↓LV torsion ↑LV and RV MPI'	↑LV CO ↑IVS S' ↑LV and RV IVCT'	↑LV and RV IVRT' ↓LV E'/A' (<1) ↓RV/E'/A' (<1)

FGR, fetal growth restriction; LV, left ventricle; RV, right ventricle; IVS, interventricular septum; S, strain; SR, strain rate; L-S, longitudinal strain; L-SR, longitudinal systolic strain rate; CO, cardiac output; S', systolic myocardial velocity; E'/A', early diastolic myocardial velocity to late atrial contraction myocardial velocity ratio derived by PW-TDI technique; MPI', myocardial performance index; IVCT', isovolumetric contraction time by PW-TDI; IVRT', isovolumetric relaxation time by PW-TDI; ↑, increased; ↓, decreased.

FIGURE LEGENDS

Figure 1 Cardiac geometry in FGR and normal term fetuses and neonates. Box-and-whisker plots demonstrate significant alterations in (A) RV sphericity index and (B) LV sphericity index in FGR groups compared to normal controls (normal fetuses and neonates are shown in *white,* FGR groups are in *black*). Boxes represent median and interquartile range, and whiskers are 5^{th} and 95^{th} centiles; Sphericity index = ventricular end-diastolic dimension/end-diastolic length; *, p-value < 0.001 and †, p-value <0.01.

Figure 2 Myocardial deformation and myocardial performance index alterations in FGR and normal term fetuses and neonates. (A) Speckle tracking myocardial deformational curve showing LV longitudinal strain rate in FGR term fetus with the systolic peak [s], early diastolic peak [e] and late atrial contraction peak [a]. Box-and-whisker plots demonstrate (B) RV longitudinal strain [L-S] and (C) RV myocardial performance index' [MPI'] in FGR fetuses and neonates compared to normal groups (normal fetuses and neonates are shown in *white,* and FGR groups are in *black*). Boxes represent median and interquartile range, and whiskers are 5^{th} and 95^{th} centiles; *, p-value < 0.001 and †, p-value <0.01. Deformational values are normalised by ventricular length.

Figure 3 Association of LV rotational indices with cardiac parameters in FGR term fetuses. Scatter plots showing a significant linear correlation of (A) LV torsion with LV apical circumferential strain (C-S) [R^2=0.74, p=0.001] and (B) LV apical systolic rotation with LV apical radial strain rate (R-SR) [R^2=0.62, p=0.001] in FGR term fetuses. Strain values are normalised by ventricular length.

Figure 4 Summary of cardiac geometrical and functional alterations in FGR fetuses and neonates compared to normal controls. Spiderweb plot showing significant alterations of cardiac parameters in FGR term fetuses *(blue)* and FGR neonates *(red)* compared to normal controls *(green)*. LV, left ventricular; RV, right ventricular; SI, sphericity index; L-SR, longitudinal strain rate; IVCT', isovolumetric contraction time; IVRT', isovolumetric relaxation time; S', myocardial systolic velocities.

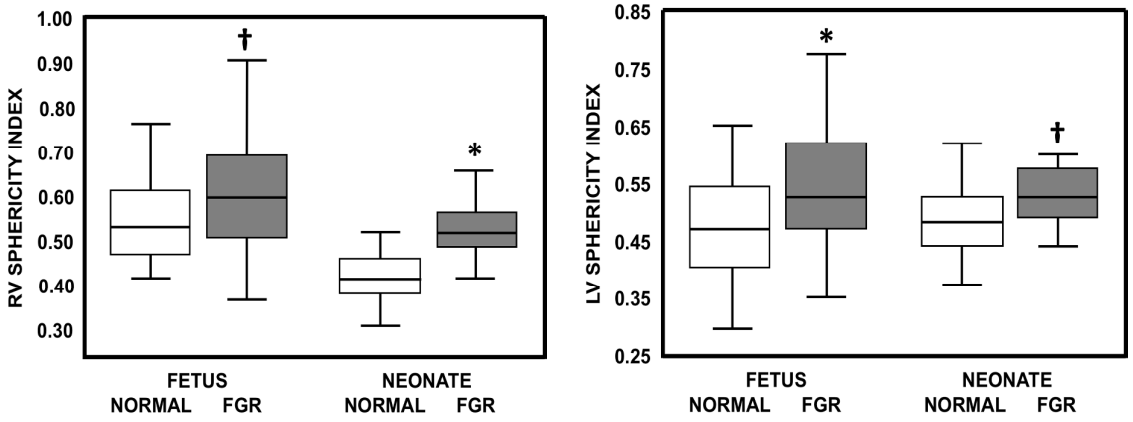

A. **B.**

Figure 1.

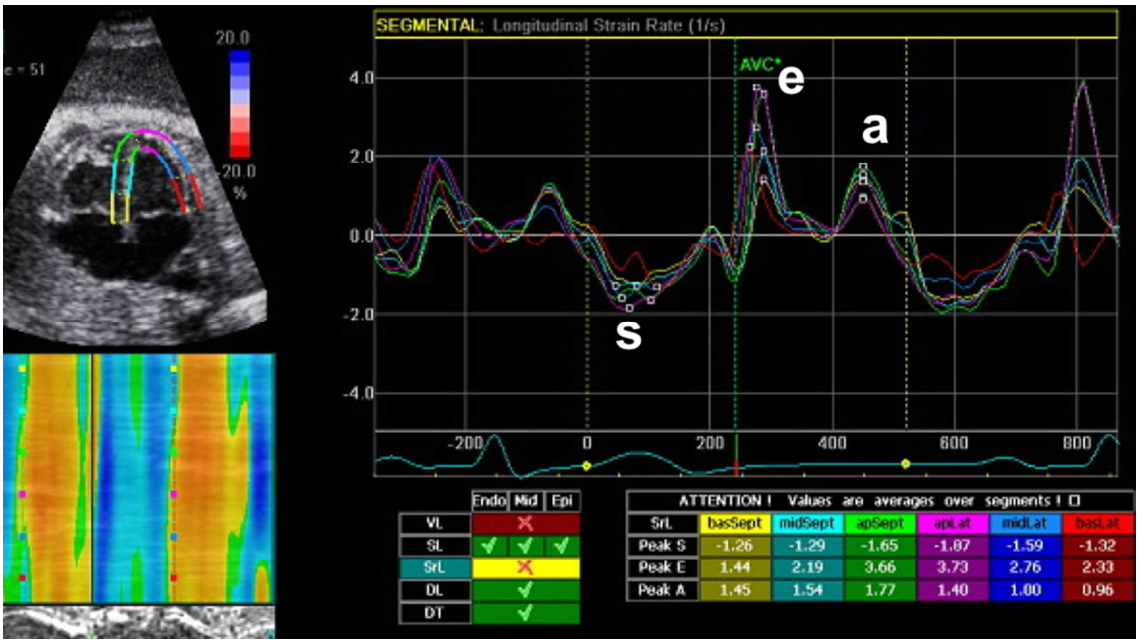

A.

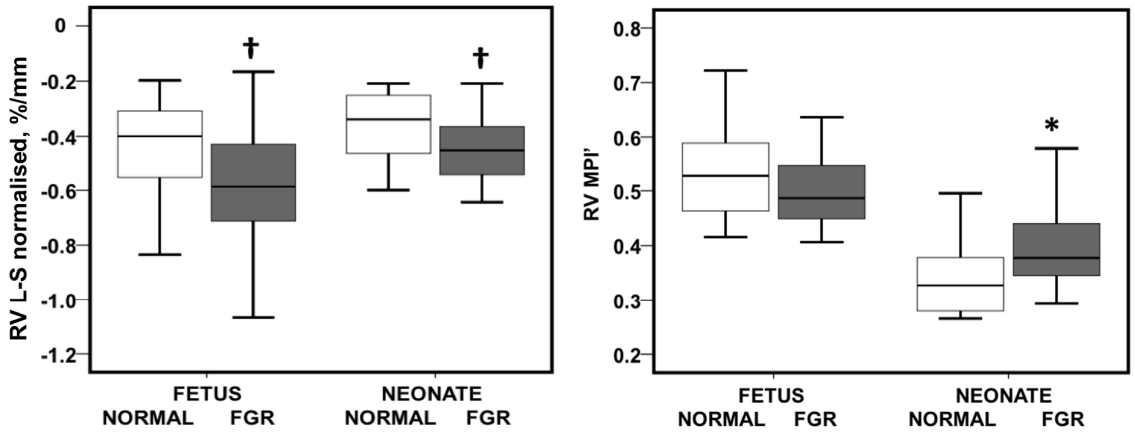

B. C.

Figure 2.

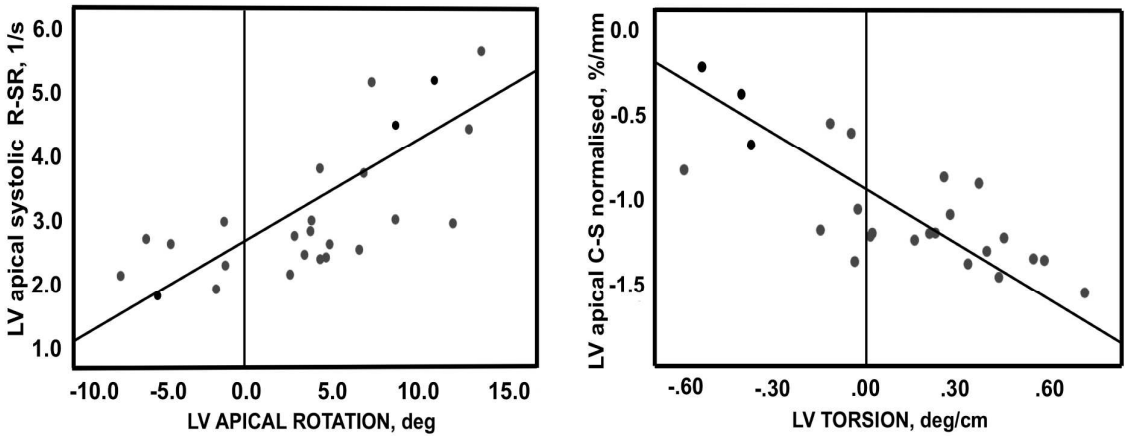

A. **B.**

Figure 3.

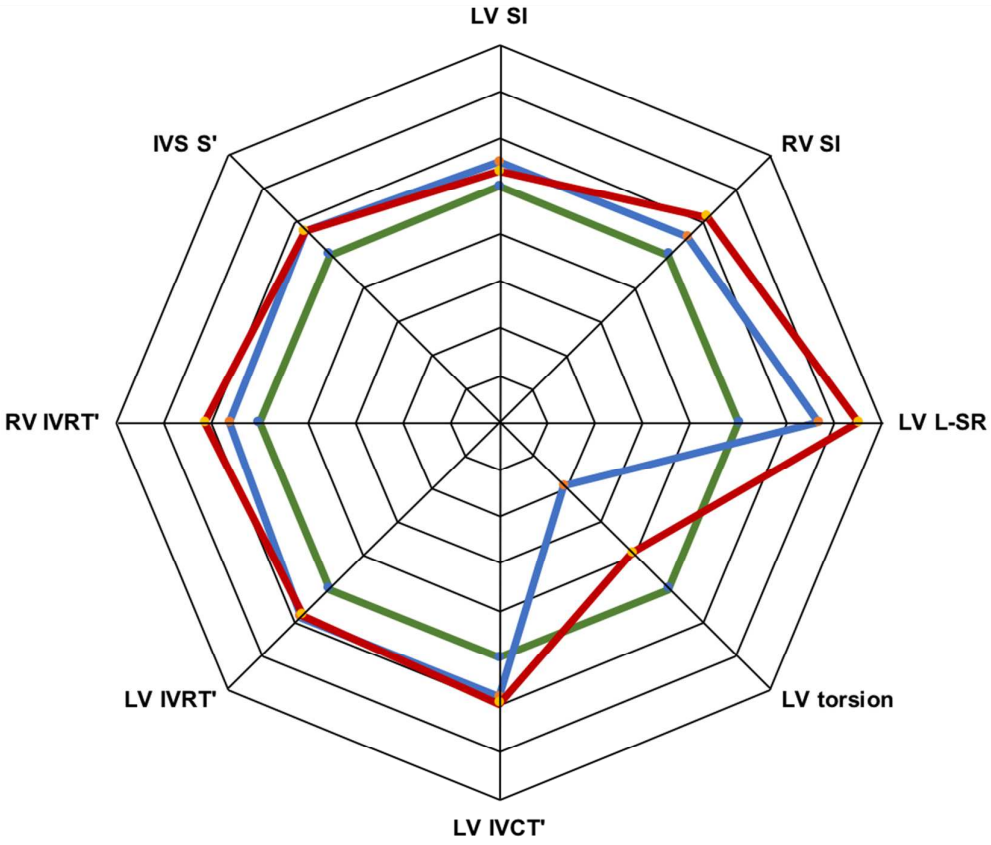

Figure 4.